The Journal of Experimental Biology 206, 117-129

doi:10.1242/jeb.00053

Differential expression of voltage-sensitive K^+ and Ca^{2+} currents in neurons of the honeybee olfactory pathway

Bernd Grünewald

Institut für Biologie, Neurobiologie, Freie Universität Berlin, Königin-Luise-Strasse 28/30, D-14195 Berlin, Germany

e-mail: gruenewa@neurobiologie.fu-berlin.de

Accepted 26 September 2002

Summary

In order to understand the neuronal processes underlying olfactory learning, biophysical properties such as ion channel activity need to be analysed within neurons of the olfactory pathway. This study analyses voltage-sensitive ionic currents of cultured antennal lobe projection neurons and mushroom body Kenyon cells in the brain of the honeybee *Apis mellifera*. Rhodamine-labelled neurons were identified *in vitro* prior to recording, and whole-cell K^+ and Ca^{2+} currents were measured. All neurons expressed transient and sustained outward K^+ currents, but Kenyon cells expressed higher relative amounts of transient A-type K^+ ($I_{K,A}$) currents than sustained delayed rectifier K^+ current ($I_{K,V}$). The current density of the $I_{K,V}$ was significantly higher in projection neurons than in Kenyon cells. The voltage-dependency of K^+ currents at positive membrane potentials was linear in Kenyon cells, but N-shaped in projection neurons. Blocking of voltage-sensitive Ca^{2+} currents transformed the N-shaped voltage-dependency into a linear one, indicating activation of calcium-dependent K^+ currents ($I_{K,Ca}$). The densities of currents through voltage-sensitive Ca^{2+} channels did not differ between the two neuron classes and the voltage-dependency of current activation was similar. Projection neurons thus express higher calcium-dependent K^+ currents. These analyses revealed that the various neurons of the honeybee olfactory pathway *in vitro* have different current phenotypes, which may reflect functional differences between the neuron types *in vivo*.

Key words: patch clamp, mushroom body, antennal lobe, insect, calcium-dependent K^+ current, honeybee, *Apis mellifera*, neuron, olfactory.

Introduction

The formation of olfactory memory is a multistage process that involves different areas of the insect brain. Olfactory conditioning of the proboscis extension reflex of the honeybee has proved to be a very powerful system for studying learning-related neural mechanisms, enabling major neural elements of the olfactory and reward pathways in the honeybee brain to be identified (Erber et al., 1980; Hammer, 1993; Mauelshagen, 1993; Grünewald, 1999b; Hammer and Menzel, 1998) (for reviews, see Hammer, 1997; Menzel, 1999, 2001) and several molecular pathways involved in this behaviour to be elucidated (e.g. Hildebrandt and Müller, 1995; Müller, 1996, 2000; Grünbaum and Müller, 1998; Fiala et al., 1999) (for a review, see Menzel and Müller, 1996). Odors are perceived by sensillae on the honeybee antennae. The axons of the olfactory receptor neurons terminate within the primary olfactory neuropils of the honeybee brain, the antennal lobes. Olfactory information is processed here in a complex spatio–temporal fashion (Joerges et al., 1997; Stopfer et al., 1997; Sachse et al., 1999) and projection neurons transmit olfactory information from the antennal lobes to the lateral protocerebral lobes and the mushroom bodies within the protocerebrum (Homberg, 1984; Fonta et al., 1993; Abel et al., 2001). In the mushroom body calyces the projection neurons synapse onto mushroom body-intrinsic Kenyon cells, named after their discoverer (Kenyon, 1896). Olfactory information converges here with information from other sensory modalities, such as visual input in the mushroom body, and with reward-processing modulatory neurons from the suboesophageal ganglion (Erber et al., 1987; Hammer and Menzel, 1995). Intracellular recordings showed that odor applications induce complex spiking patterns in projection neurons, thus encoding olfactory and gustatory sensory information (Stopfer et al., 1997; Abel et al., 2001; Müller et al., 2002). The underlying ion channels of projection neurons have not yet been analysed, however, because the neurons could not be identified and distinguished from local interneurons, as is possible in other insects (Hayashi and Hildebrand, 1990; Oland and Hayashi, 1993).

The ionic currents of postsynaptic Kenyon cells, by contrast, have been analysed *in vitro*. They express functional nicotinic acetylcholine receptors, which may mediate fast synaptic transmission between antennal lobe projection neurons and mushroom body Kenyon cells (Goldberg et al., 1999; Deglise

et al., 2002). Several voltage-sensitive ionic currents have been described (Schäfer et al., 1994; Pelz et al., 1999). Among the three different voltage-sensitive K^+ currents is a transient A-type K^+ current, which resembles the shaker-like current of other systems and interacts with a fast voltage-sensitive Na^+ current during spike generation (Pelz et al., 1999). Similar voltage-sensitive currents have been described in honeybee antennal motor neurons, both *in vitro* and *in situ* (Kloppenburg et al., 1999a).

The antennal lobes and mushroom bodies are differentially involved in memory formation in the honeybee (Erber et al., 1980; Hammer and Menzel, 1998; Menzel, 2001) and our long-term goal is to analyse learning-related changes of cell physiology in the different olfactory neurons, beginning with an analysis of the ionic conductances of the different neurons types, antennal lobe projection neurons and mushroom body Kenyon cells. This, however, requires a staining technique that allows the identification of the neuron type prior to recording. Whereas cultures of mushroom bodies comprise somata of a homogeneous cell type (Kenyon cells), the dissociation of antennal lobes yields a heterogeneous mixture of projection neurons and local interneurons (Gascuel and Masson, 1991b; Devaud et al., 1994; Kirchhof and Mercer, 1997). To record from identified cell types, namely projection neurons and Kenyon cells, we have developed a labelling technique that enabled us to identify neurons in the culture dish prior to patch clamp recording. This study revealed pronounced differences between projection neurons and Kenyon cells.

Materials and methods

Animals and neuron labelling

Honeybee *Apis mellifera* L. pupae were collected from the comb between days 4 and 6 of pupal development, which lasts 9 days under natural conditions. At these stages projection neurons have already formed a branching pattern in the antennal lobe and the mushroom body, which is very similar to adult cell morphology (Schröter and Malun, 2000).

Projection neurons were identified by dye injection. For this, dextran-coupled rhodamine (MW 3000, Molecular Probes Inc., Eugene, OR, USA) was injected into the mushroom body calyces (see below), and the somata of projection neurons from the antennal lobes were retrogradely labelled and could easily be identified *in vitro* (see below). The procedure used was a modification of a protocol developed for confocal microscopical analyses of projection neuron morphology (Schröter and Malun, 2000).

Pupal honeybees were decapitated and a small window was cut into the head cuticle frontally between the compound eyes, the bases of the antennae, and the ocelli. After removal of trachea and glands the brain, with the prominent mushroom body calyces, was clearly visible. The head was flooded with sterile standard external saline (see below) with gentamycin (150 µl/50 ml, Gibco Life Technologies, Karlsruhe, Germany) added. Using a sterile quartz glass capillary (1.0 mm o.d., 0.5 mm i.d.) pulled with a horizontal laser puller (P2000, Sutter Instruments, Novato, CA, USA), the lip region of the calyces was repeatedly punctured in order to damage the neurons and allow dye uptake. A saturated paste from the dextran-coupled rhodamine was prepared by adding one drop of sterile distilled water to the dry dextran–rhodamine on a glass slide. Therefore, the exact dye concentration could not be determined. The lip regions of the calyces were briefly punctured with a sterile capillary, whose tip was coated with the paste, to insert a small amount of dye. After gently rinsing off excessive dye solution with standard external saline, the dye was allowed to diffuse to the somata for 3 h at room temperature.

Confocal microscopy

To confirm that rhodamine–dextran labelled only projection neurons in the antennal lobe, whole-mount preparations were analysed using confocal microscopy. Brains were dissected out of the head capsule after labelling, briefly rinsed with standard external saline, and fixed for 1 h in 4% paraformaldehyde in 0.1 mol l^{-1} phosphate-buffered saline (PBS), pH 7.2 at room temperature. Subsequently, specimens were dehydrated in graded ethanol and cleared in methyl salycilate. Whole-mounts were mounted in Permount (Fisher Chemicals, Springfield, NJ, USA) on slides and viewed with a confocal laser scanning microscope (Leica TCS-4D) equipped with a krypton/argon laser light source. At primary magnifications between 10–40×, several optical sections were imaged at 1–5 µm intervals. Series of images were stacked and two-dimensional projections of image stacks generated using the extended focus function of Imaris software (version 2.7, Bitplane).

Preparation of cell cultures and cell identification in vitro

Kenyon cells and projection neurons were dissected and cultured following a modified protocol of Kreissl and Bicker (1992). After the staining procedure brains were removed from the head capsule and transferred into a preparation medium (Leibovitz L15, Gibco BRL; see below). The glial sheath was gently removed and the mushroom bodies or the antennal lobes dissected out of the brains. After incubation (10 min) in calcium-free saline, mushroom bodies were transferred back to the preparation medium (2 mushroom bodies or 10–15 antennal lobes per 100 µl medium) and dissociated by gentle trituration with a 100 µl Eppendorf pipette. Cells were then plated in 10 µl samples on Falcon plastic dishes coated with polylysine (polylysine-L-hydrobromide, MW 150–300 kDa, Sigma) and allowed to settle and adhere to the substrate for at least 15 min. Thereafter, the dishes were filled with 2.5 ml of a supplemented culture medium (see below) and were kept at 26°C in an incubator at high humidity. Because the mushroom bodies can be mechanically dissected out of the brain and contain somata of Kenyon cells exclusively, this procedure yielded a culture of pure Kenyon cells. By contrast, antennal lobe neurons are a heterogeneous population consisting of two major classes, projection neurons and local interneurons. Thus, dissection of antennal lobes yielded cultures containing neurons of different classes (cf. Kirchhof and Mercer, 1997) and projection neurons needed to be identified *in vitro*. Since

only projection neurons were labelled by dextran–rhodamine, their somata were easily identified in the culture dish by their fluorescence. Labelled projection neurons were located with epifluorescence illumination and photographed using a Zeiss inverted microscope (Axiovert 10, Zeiss, Jena, Germany), which was part of the patch clamp setup. Images were taken under phase-contrast optics at 32× primary magnification with a PC-controled digital camera (Olympus DP10; utility software C-2.1, Olympus). The digitized images were analysed and processed with Adobe Photoshop (version 5.0, Adobe Systems Inc.).

For electrophysiological measurements, cells were used between culture days 3 and 6. Processes of those cells chosen for recordings did not overlap with neighbouring neurites.

The contents of the cell culture solutions were similar to those used during earlier physiological studies (Goldberg et al., 1999; Pelz et al., 1999).

Preparation medium

To 1000 ml of Leibovitz's L15 medium (Gibco) was added: sucrose, 30.0 g; glucose, 4.0 g; fructose, 2.5 g; proline, 3.3 g. The medium was adjusted to pH 7.2 with NaOH and to 500 mosmol l^{-1} with sucrose.

Culture medium

Culture medium contained heat-inactivated fetal calf serum (Sigma, St Louis, MO, USA),13% (v/v); yeast hydrolysate (Sigma), 1.3% (v/v); L-15 powder medium (Gibco BRL), 12.5% (w/v); glucose, 18.9 mmol l^{-1}; fructose, 11.6 mmol l^{-1}; proline, 3.3 mmol l^{-1}; 93.5 mmol l^{-1} sucrose; Pipes, 2.1 mmol l^{-1}. The medium was adjusted to pH 6.7 and 500 mosmol l^{-1}.

Calcium-free saline

Calcium-free saline consisted of: NaCl, 147 mmol l^{-1}; KCl, 5 mmol l^{-1}; Hepes, 65 mmol l^{-1}; pH 7.2, 392 mosmol l^{-1}.

Electrophysiology

Whole-cell seal recordings (GΩ) were performed at room temperature following the methods described by Hamill et al. (1981). Recordings were made using a computer-controlled HEKA EPC9 patch-clamp amplifier (HEKA-Elektronik, Lambrecht, Germany). Data acquisition and online analyses were performed with PULSE software (version 8.50, Heka-Elektronik) running on a Pentium-based PC. Data were sampled at 10–20 kHz and were low-pass filtered with a four-pole Bessel filter. Voltages were corrected for liquid junction potential (4 mV); leakage currents were not subtracted. Series resistances were 5–20 MΩ and were compensated at about 80%. The cell capacitance for each cell was estimated from the capacitance compensation routine of the PULSE software. For some cells, cell capacitances and time constants were calculated from capacitive charging currents, which were measured during hyperpolarizing voltage pulses to a nonactive region of the membrane potential (–80 to –100 mV) prior to capacitance compensation. Electrodes were pulled from borosilicate glass capillaries (GB150-8P, Science Products Germany) with a horizontal puller (DMZ Zeitz Instruments, München, Germany), and had tip resistances of 8–12 MΩ in standard external solution (see below). The holding potential was –80 mV throughout.

Solutions

The bath was continuously perfused at about 2 ml min^{-1} with a standard external solution that consisted of NaCl, 130 mmol l^{-1}; KCl, 6 mmol l^{-1}; $MgCl_2$, 4 mmol l^{-1}; $CaCl_2$, 5 mmol l^{-1}; sucrose, 160 mmol l^{-1}; glucose, 25 mmol l^{-1}; Hepes, 10 mmol l^{-1}. The external saline was adjusted to pH 6.7 with NaOH and to 510 mosmol l^{-1}. To record currents through K^+ channels, the standard saline was replaced with one in which tetrodotoxin (TTX, 100 nmol l^{-1}) was added to block currents through the voltage-sensitive Na^+ channels. Some experiments were performed with additional $CdCl_2$ (50 μmol l^{-1}) in the external solution to block voltage-sensitive Ca^{2+} currents. The pipette solution contained: K-gluconate, 87 mmol l^{-1}; KF, 40 mmol l^{-1}, KCl, 20 mmol l^{-1}; $CaCl_2$, 0.2 mmol l^{-1}; $MgCl_2$, 3 mmol l^{-1}; K-EGTA, 10 mmol l^{-1}; Na_2ATP, 3 mmol l^{-1}; Mg-GTP, 0.1 mmol l^{-1}; glutathione, 3 mmol l^{-1}; sucrose, 120 mmol l^{-1}; Hepes/bis-Tris, 10 mmol l^{-1}; pH 6.7, 500 mosmol l^{-1}. To record currents through Ca^{2+} channels, tetraethylammonium chloride (TEA-Cl, 10 mmol l^{-1}) was added to the external standard saline. In the pipette solution K^+ ions were replaced by TEA or Cs^{2+}; Cs-gluconate, TEA-Cl, Cs-EGTA and CsF replaced the corresponding K^+ salts. All chemicals were purchased from Sigma (St. Louis, MO, USA).

Data analyses

Patch clamp data were analysed with PulseFit software (version 8.5, Heka) and Igor Pro (version 3.12; WaveMetrics Inc, OR, USA) on a Pentium-based PC. Statistical analyses were performed using Statistica (version 5.1, StatSoft Inc., Tulsa, OK, USA). Values are given as means ± standard errors of means (S.E.M.). Statistical significances between means were tested using Student's *t*-test; the level of significance was taken as $P=0.05$.

Results

Morphological identification of projection neurons

The staining procedure labelled somata and neurites of intrinsic and extrinsic mushroom body neurons, including axonal branches of antennal lobe projection neurons. The somata of projection neurons are located within the rim around the antennal lobes (Fig. 1). Whole-mount analyses revealed that rhodamine–dextran labelling of the axonal terminals yielded from 50 to several hundred stained somata in each antennal lobe. Each projection neuron sends one primary neurite into the neuropilar area of the antennal lobe, where it forms glomerular arborizations. The antennocerebralis tracts (ACT), which connect the antennal lobe with the protocerebrum, are densely stained. Neurites running within

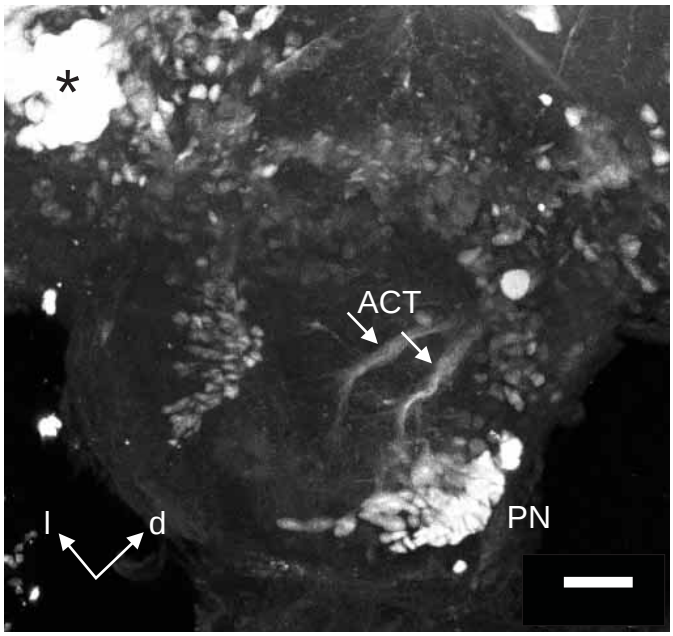

Fig. 1. Confocal micrograph of the honeybee antennal lobe with labelled projection neurons. Injections of dextran-coupled rhodamine into the mushroom bodies stained projection neurons (PN); their somata are clustered around the antennal lobe. In this specimen only the median cluster was labelled, but in other preparations the other clusters around the antennal lobe were also labelled. The roots of the antennocerebralis tracts (ACT) are also stained (arrows). Within the protocerebrum the somata of mushroom body feedback neurons within a lateral cluster are densely stained (asterisk), because they innervate all calycal regions. Frontal view of a whole-mount preparation; lateral (l) and dorsal (d) directions are indicated. Scale bar, 50 μm.

the median or the lateral ACT are labelled. Thus, somata of both ACT neurons were cultured.

Within the protocerebrum other mushroom body-extrinsic neurons, which innervate the mushroom bodies are stained as well. Among these neurons, feedback neurons form extensive branches within all calycal regions (Grünewald, 1999a). Accordingly, feedback neurons are well stained by rhodamine–dextran; two somata clusters were visible in most specimens. In addition, the dye labelled numerous Kenyon cells in each mushroom body. Cultures prepared from mushroom bodies contain only somata of Kenyon cells and some of them were labelled. In cultures prepared from antennal lobes only projection neurons were labelled, because only the antennal lobes were dissected out of the brain, and the somata of other mushroom body-extrinsic neurons, such as feedback neurons, were not cultured.

Outgrowth of olfactory projection neurons and Kenyon cells in vitro

All cells were treated identically before, during and after the neurons were cultured. For cultures of Kenyon cells the yield from one mushroom body was plated onto 10 dishes, and the yield from 2–3 antennal lobes plated onto one dish. Thus, the cell density of the Kenyon cell and the projection neuron cultures were similar and adjusted so that the neurites of individual neurons did not overlap. The labelling remained visible in cultured neurons, allowing cell identification throughout the period of observation. Within each dish, 2–10 labelled projection neurons (or numerous Kenyon cells) were identified after 2–6 days *in vitro*. Neurons started to sprout new and fine processes after 1 day *in vitro* and continued to grow until day 6, the last day of observation (Fig. 2). The somata diameters of cultured Kenyon cells measured approximately 7–10 μm, as in the intact pupal mushroom body. The diameters of somata from projection neurons were larger (10–25 μm), similar to their size in the intact brain (Schröter and Malun, 2000), and the area covered by their branches were larger than those of Kenyon cells. Individual branches of cultured honeybee neurons were very thin, especially those of Kenyon cells, with a diameter of less than 1 μm. We did not quantify potential morphological differences between the neuron types *in vitro*, because most neurons were used for electrophysiological experiments before they grew elaborate neuritic branches.

Potassium currents

Whole-cell patch clamp recordings were performed from projection neurons, identified from their fluorescence, and from Kenyon cells, which were derived from pure mushroom body cultures. Cells were measured electrophysiologically *in vitro* between days 3 and 5. Older neurons had rather elaborate neuritic branches, which would compromise the control of the membrane potential (space clamp). Thus, a total of 53 cells (22 Kenyon cells, 31 projection neurons) were measured. The capacitance of Kenyon cells was 4.1±0.27 pF (N=22) and 11.30±0.68 pF for projection neurons (N=31). Kenyon cells have significantly smaller cell capacitances because of their smaller somata diameters (P<0.001, t=–8.56, d.f.=51, Student's t-test).

From the holding potential of –80 mV a hyperpolarizing prepulse was applied to –120 mV to completely remove inactivation of the transient A type K^+ current (cf. Pelz et al., 1999). Whole-cell membrane currents induced by depolarizing voltage pulses of Kenyon cells and projection neurons were dominated by large voltage-sensitive outward currents (Fig. 3). Depolarizing voltage pulses also induced a rapidly activating transient inward current in most cells, which was blocked in all experiments by switching to an external saline containing 100 nmol l^{-1} TTX. Kenyon cells and projection neurons expressed different types of outward K^+ currents. Schäfer et al. (1994) identified that these outward currents are carried by K^+ ions, by altering the external K^+ concentration and determining the tail current reversal potential. The outward K^+ currents may comprise a rapidly activating transient and a sustained component (delayed rectifier, $I_{K,V}$). The transient K^+ current (A type current, $I_{K,A}$) of the Kenyon cells was more pronounced than the $I_{K,A}$ of the projection neurons, as can be seen when comparing traces of typical currents of two representative cells (Figs 3, 5). The transient current

component can be blocked in Kenyon cells by a depolarising prepulse to –20 mV (Pelz et al., 1999). Accordingly, inactivating prepulses reduced the amplitude of the transient K^+ currents in Kenyon cells, but did not affect whole cell K^+ currents of projection neurons (Fig. 3). Subtraction of these currents yielded the pure transient K^+ current (Fig. 3C). The $I_{K,A}$ was a large portion of the total K^+ current of Kenyon cells, whereas such transient K^+ currents were negligible in projection neurons. The ratio of transient over sustained K^+ current, as revealed by calculating the quotient of the maximum current at the current onset and at the end of the depolarizing pulse (command potential +50 mV), was higher in Kenyon cells than in projection neurons (P<0.0001, t=8.95, d.f.=30, Student's t-test, N=10 Kenyon cells, 22 projection neurons; Fig. 4C).

The K^+ current amplitudes of the projection neurons were higher than those of Kenyon cells (Fig. 4A). Measured at a pulse potential of +50 mV, the mean peak outward current (measured a few ms after current onset) of projection neurons measured 7376.5±117.2 pA and was significantly higher than those of Kenyon cells (2907.2±67.1 pA; P<0.001, t=3.65, d.f.=30, Student's t-test). Similarly, when measured at the end of the depolarizing pulse, the amplitude of the sustained current component was higher in projection neurons (P<0.001). This was only partially due to the larger soma diameter of projection neurons, since the comparison of the current densities (pA/pF) revealed differences for the sustained K^+ current (567.0±46.0 pA/pF for projection neurons *versus* 326.9±50.2 pA/pF for Kenyon cells, P<0.005, t=3.18, d.f.=29), but not for the transient K^+ current (Fig. 4B, P=0.29). This indicates that the total K^+ current consisted mainly of non-inactivating currents and only a small transient component, whereas that of Kenyon cells was a mixture of inactivating and non-inactivating currents with a pronounced transient current.

The I-V relationship of the outward currents showed current activation at approximately –45 mV (Figs 5C, 6). The I-V curves of projection neurons and Kenyon cells differed when whole-cell currents were measured without blockade of the calcium currents by external Cd^{2+}. Kenyon cells expressed a linear voltage-dependency of K^+ currents at positive membrane potentials. By contrast, projection neurons showed a pronounced N-shaped I-V curve with a local current peak at +60 mV and a local minimum at +80 mV (Figs 5C, 6). When voltage-sensitive Ca^{2+} currents were blocked with external 50 μmol l^{-1} Cd^{2+} the outward currents of projection neurons were significantly reduced. By contrast, Cd^{2+} did not affect or only slightly increased the outward K^+ currents of Kenyon cells (Fig. 5B,C). In addition, external Cd^{2+} irreversibly transferred the N-shaped form of the I-V curve of projection neurons into a linear one (Fig. 5C), indicating that Cd^{2+} blocked a calcium-sensitive outward current in projection neurons but not in Kenyon cells. Typically, such a calcium-dependent N-shaped I-V curve is caused by the activation of calcium-dependent K^+ currents.

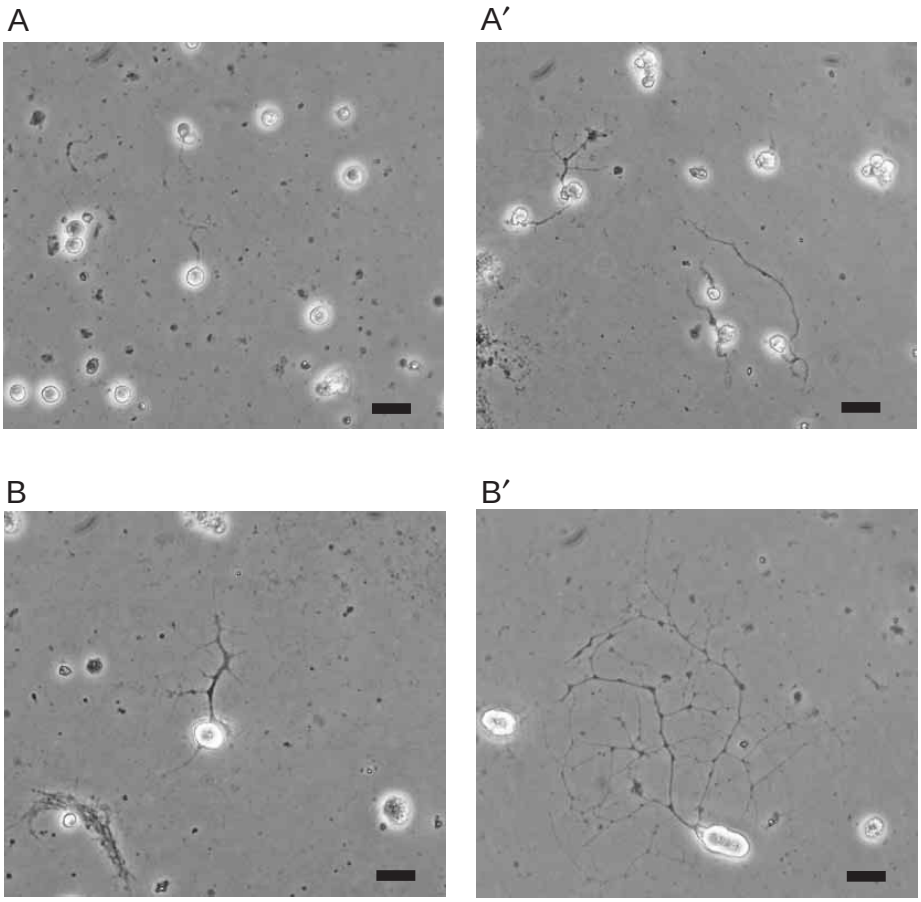

Fig. 2. Outgrowth of Kenyon cells (A,A′) and projection neurons (B,B′) after 2 (A,B) and 6 (A′,B′) days in primary cell culture. The neurons start to grow processes after 1 day *in vitro*. These neurites continue growing and branching throughout the period of 1 week. The somata diameters of projection neurons are larger and they grow longer neurites with more branches. Phase contrast; primary magnification 32×. Scale bars, 20 μm.

Calcium currents

The differences in Ca^{2+}-dependent K^+ currents may reflect differences in the voltage-sensitive Ca^{2+} currents. Therefore, we measured the voltage-sensitive Ca^{2+} currents of Kenyon cells and projection neurons. For this, currents through calcium channels were isolated by blocking outward K^+ currents with external TEA and Cs^{2+} in the patch pipette and voltage-sensitive Na^+ currents with external TTX. The remaining inward currents were currents through Ca^{2+} channels (Schäfer

et al., 1994). Under these conditions, depolarizing command potentials activated inward currents at command potentials higher than –40 mV in both neuron types (Figs 7, 8). These currents through calcium channels showed rapid activation and slow inactivation (Fig. 7A). The peak current amplitude ranged between –38.6 and –419.9 pA (mean –197.3±30.9 pA, *N*=12) for Kenyon cells. Projection neurons expressed Ca^{2+} currents with peak amplitudes of –292.6 to –1166.2 pA (mean –683.0±30.9 pA, *N*=9, Fig. 8B). When equimolar barium was used a charge carrier instead of calcium, the whole-cell currents through calcium channels did not change substantially (not shown). Instead, current amplitudes were only slightly increased and the current decay during depolarizing was almost indistinguishable (not shown). The Ca^{2+} currents were sensitive to externally applied 50 µmol l^{-1} Cd^{2+}, a concentration that was shown to be sufficient to completely and irreversibly block Ca^{2+} currents in Kenyon cells (Schäfer et al., 1994). However, in projection neurons, a small Cd^{2+}-resistant inward current remained unblocked at this Cd^{2+} concentration (Fig. 7B).

The voltage threshold for activation of inward Ca^{2+} currents was approximately –35 mV. The current–voltage relationship of the currents through Ca^{2+} channels peaked at command potentials between 0 and 10 mV and had a reversal potential at

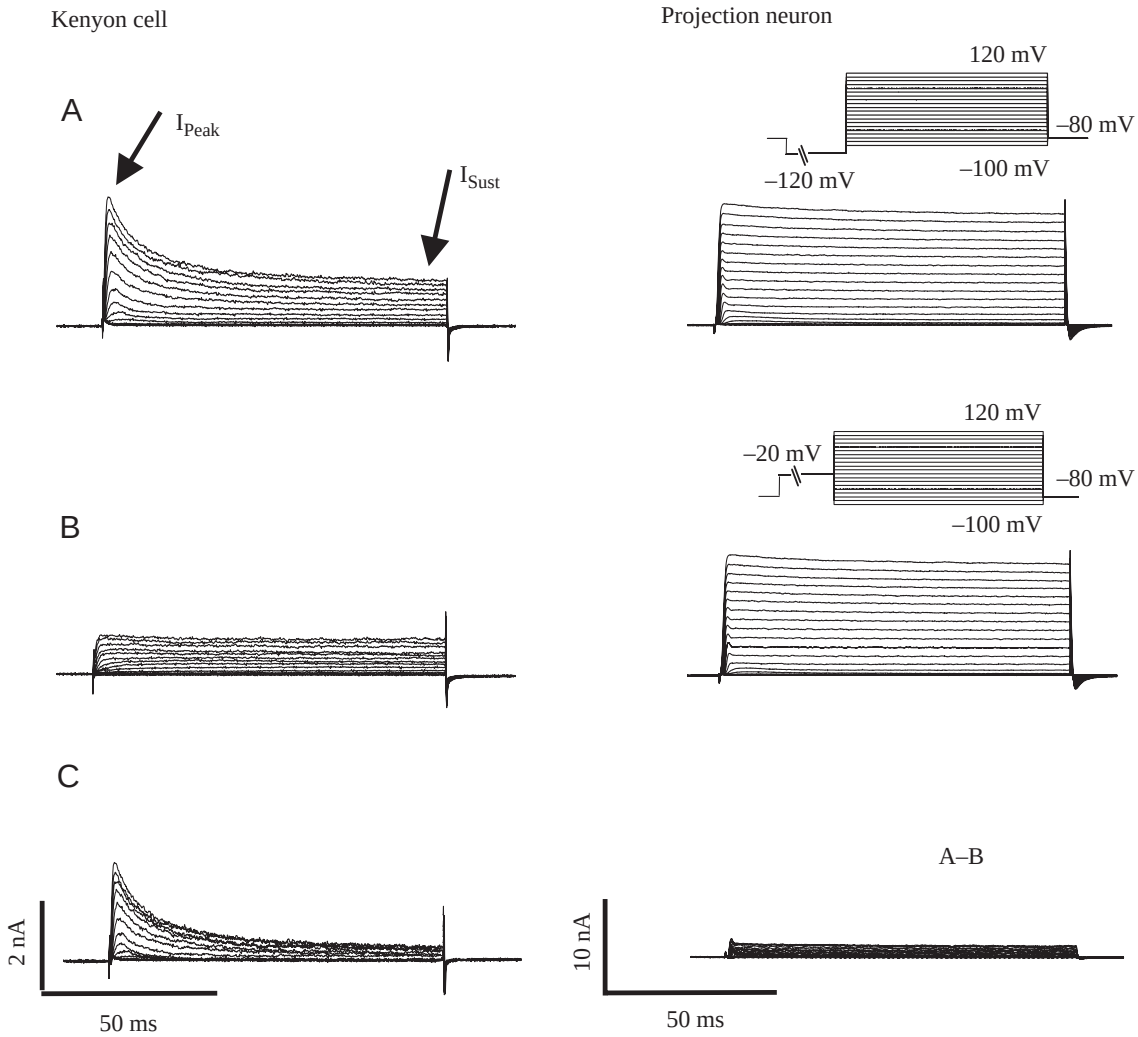

Fig. 3. Different levels of transient K^+ currents. Typical examples of voltage-sensitive currents of a Kenyon cell (left) and a projection neuron (right) are shown. (A) In the presence of tetrodotoxin (TTX) and Cd^{2+} in the external saline to block currents through voltage-sensitive Na^+ and Ca^{2+} channels, voltage-sensitive outward currents were isolated. Activation protocols for the experiments: cells were held at –80 mV. To remove channel inactivation, a long conditioning pulse to –120 mV (1 s) (cf. Pelz et al., 1999) preceded depolarizing voltage commands (potentials from –100 to +120 mV, 10 mV increments, duration 100 ms). Under these conditions Kenyon cells expressed a prominent inactivating K^+ current (I_{Peak}), which was less pronounced in projection neurons, where a sustained K^+ current (I_{Sust}) dominated. Arrows indicate time points where currents were measured in the other figures and they point to the peak current (I_{Peak}) and to the sustained current (I_{Sust}) at the end of the voltage pulse. (B) Following an inactivating prepulse to –20 mV (1 s), the transient K^+ current of Kenyon cells was completely inactivated during depolarising pulses to various command potentials, whereas the outward currents of projection neurons remained relatively unaffected. (C) Subtracting trace B from trace A gave the amount of inactivating K^+ current in the two neurons. Note the different scale bars for Kenyon cells and projection neurons.

approximately 35–45 mV (Figs 7C, 8A). The overall shapes of the voltage-sensitive Ca^{2+} currents and the I-V curves of this current in Kenyon cells and projection neurons were similar (Fig. 8A). The mean peak current amplitudes, however, were significantly higher in projection neurons than in Kenyon cells (P<0.0001, t=–5.57, d.f.=19, Student's t-test; Fig. 8B). This is probably due to their larger soma diameter, because the mean peak Ca^{2+} current densities (pA/pF) did not differ (P=0.29, t=–1.09, d.f.=19; Fig. 8C). Thus, Kenyon cells and projection neurons express similar voltage-sensitive Ca^{2+} currents with similar current densities.

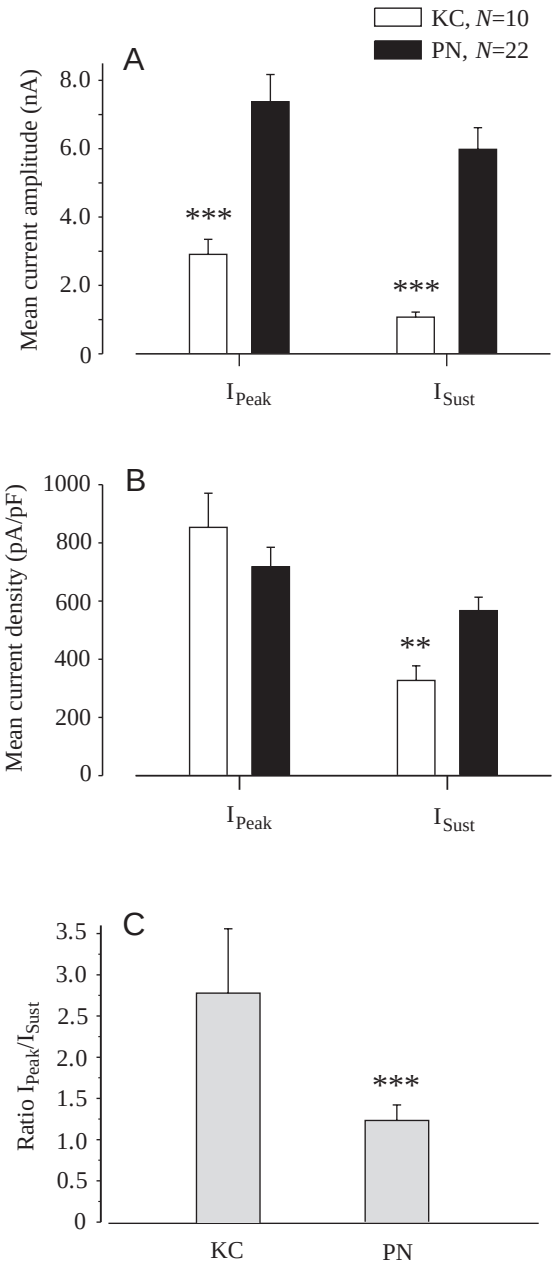

Fig. 4. Quantitative comparison of voltage-sensitive K^+ currents of Kenyon cells and projection neurons. (A) Amplitudes of K^+ currents (elicited by a depolarizing command pulse to +50 mV) measured at the peak during transient current component (I_{Peak}) and during sustained current component (I_{Sust}; arrows in Fig. 3A) are higher in projection neuron (PN) than in Kenyon cells (KC; P<0.001). (B) The mean current density of the sustained (delayed rectifier type) current (I_{Sust}) is higher in projection neurons than those of Kenyon cells (P<0.01); the current densities measured at the peak currents do not differ significantly. (C) The ratio of peak (transient) *versus* sustained K^+ current is higher in Kenyon cells (KC) than in projection neuron (PN, P<0.001). Levels of significance: *** P<0.001, ** P<0.01.

Discussion

In this study we have analysed voltage-sensitive ionic currents of identified neuron types of the honeybee brain, namely mushroom body Kenyon cells and antennal lobe projection neurons, which had been selectively labelled and identified prior to recording. The analysis revealed pronounced differences between these neurons, in particular between transient voltage-sensitive K^+ currents and a calcium-dependent K^+ current.

Identification and culturing of projection neurons

In order to assign physiological properties to a certain neuron class it is crucial to identify the neuron type. This is particularly true for antennal lobe cultures, which contain different types of neuron. Cultured projection neurons or Kenyon cells do not retain their *in vivo* morphology. This is probably not a consequence of the labelling procedure, because it has been described previously for cultures of unlabelled Kenyon cells (Kreissl and Bicker, 1992) and unidentified antennal lobe neurons (Devaud et al., 1994; Kirchhof and Mercer, 1997). Also, in the present study branching patterns of labelled and unlabelled neurons within a given culture dish were indistinguishable. Thus, in contrast to cultures of, for example, antennal lobe neurons of the moth *Manduca sexta* (Hayashi and Hildebrand, 1990; Oland et al., 1996; Mercer and Hildebrand, 2002a,b), labelling is required to differentiate between cultured local interneuron and projection neurons in the honeybee. The identification of antennal lobe projection neurons was achieved by rhodamine dye injections into the mushroom body calyces. The staining within the antennal lobes presented here is very similar to previous stainings observed with rhodamine–dextran into the mushroom body (Schröter and Malun, 2000). The morphology of the projection neurons within the honeybee brain has been described in detail elsewhere (Homberg, 1984; Gascuel and Masson, 1991a; Fonta et al., 1993; Schröter and Malun, 2000; Abel et al., 2001). The staining procedure that we used labelled other neurons as well as antennal lobe projection neurons and Kenyon cells, including several known mushroom body extrinsic neurons (Mobbs, 1982, 1985; Rybak and Menzel, 1993), mushroom body feedback neurons (Bicker et al., 1985; Grünewald, 1999a) and, occasionally, a few somata within the suboesophageal ganglia. However, staining of these neurons did not interfere with the identification of projection neurons *in vitro*, because in the antennal lobes only projection neurons could take up the tracer and were, therefore, the only labelled cells in these cultures.

Cultured dextran-labelled neurons have been used successfully for patch clamp recordings; their viability has repeatedly been noted (e.g. Kloppenburg and Hörner, 1998; Kloppenburg et al., 1999a; Dugladze et al., 2001) and was confirmed here. Projection neurons grew extensive neurites in culture throughout the period of observation (3–6 days), as has

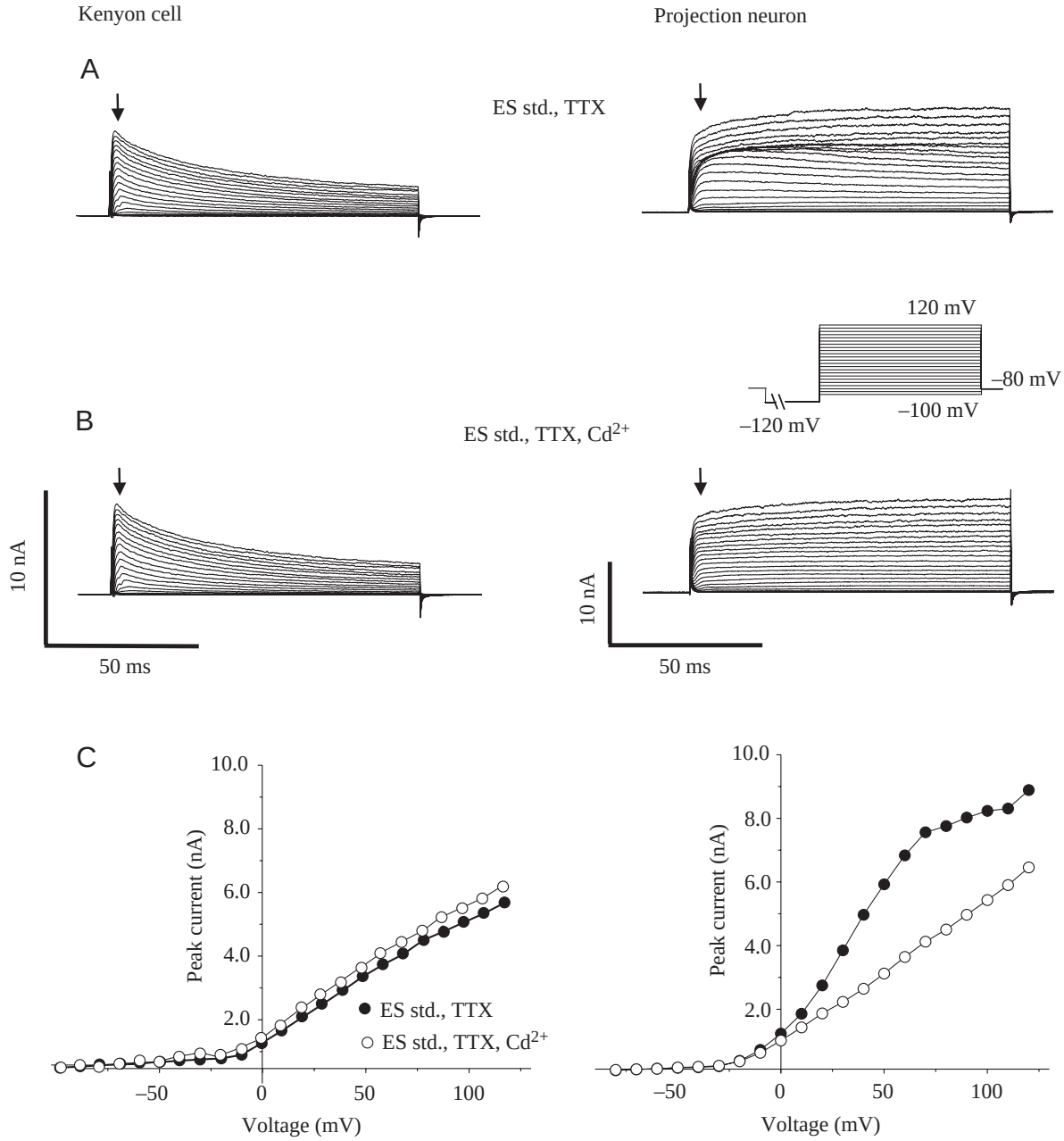

Fig. 5. Voltage- and Ca^{2+}-sensitive outward K^+ currents of a typical Kenyon cell and a projection neuron. (A) Currents were recorded in the standard external saline (ES std., see Materials and methods) with the Na^+ channel blocker tetrodotoxin (TTX, 100 nmol l^{-1}) added. As in Fig. 3, projection neurons showed higher current amplitudes (note the different scale bars) and Kenyon cells expressed prominent transient K^+ currents. Furthermore, the current amplitudes of Kenyon cells are increasing continuously with increasing depolarisations. By contrast, outward currents of projection neurons show an apparent non-linearity with a decrease of current amplitude increases between command potentials of 70–110 mV (see N-shaped I-V curve in Fig. 5C). The activation protocol for all experiments consisted of a hyperpolarising conditioning prepulse to –120 mV (1 s) and subsequent depolarizing voltage commands to various potentials (–100 to +120 mV, 10 mV increments, duration 100 ms; holding potential –80 mV). (B) Addition of the irreversible Ca^{2+} channel blocker 50 µmol l^{-1} $CdCl_2$ (Cd^{2+}) to the bath solution had little effect on K^+ currents of Kenyon cells (left), but removed non-linearity of current activation in projection neurons (right). (C) Corresponding I-V curves of the two cells showing the Cd^{2+} block of the N-shaped I-V curve for the projection neuron (right), but no significant change in the I-V curve of voltage-sensitive K^+ currents of the Kenyon cell (left). The peak currents were measured at the time points indicated by the arrows in A and B.

been described for unidentified antennal lobe neuron cultures (Gascuel and Masson, 1991a; Devaud et al., 1994; Kirchhof and Mercer, 1997), which suggests that they were healthy and that the dye did not impair the viability of the cells. The applied mass staining technique is therefore a very reliable method for the identification of honeybee antennal lobe projection neurons *in vitro* and may be used in the future for analyses of other identified neurons of the bee brain, such as mushroom body feedback neurons.

Isolation of ionic currents in identified neurons

The major finding of this study is that antennal lobe projection neurons and mushroom body Kenyon cells express different sets of ionic currents.

Kenyon cells express at least three different voltage-gated outward K^+ currents. The transient component comprises a rapidly inactivating (A-type) current and a slowly inactivating current, whose kinetic parameters have been described in great detail (Pelz et al., 1999). The amplitude of the sustained (delayed rectifier) current is relatively small compared to the transient K^+ currents, as described in various insect or crustacean neurons (e.g. Byerly and Leung, 1988; Saito and Wu, 1991; Hayashi and Levine, 1992; Delgado et al., 1998; Kloppenburg and Hörner, 1998; Benkenstein et al., 1999; Kloppenburg et al., 1999b; Schmidt et al., 2000 (for a review, see Wicher et al., 2001) and in antennal motoneurons within the honeybee deutocerebrum (Kloppenburg et al., 1999a). By contrast, projection neurons do not express such prominent transient K^+ currents. This is interesting, because computer simulations using Hodgkin–Huxley-derived equations indicated that A-type K^+ currents are mainly responsible for the membrane repolarisation during an action potential in honeybee Kenyon cells (Pelz et al., 1999; Ikeno and Usui, 1999). Similarly, *shaker* mutations in *Drosophila* impair spike repolarisation (Tanouye and Ferrus, 1985). Therefore, other outward currents (calcium-dependent or delayed rectifier currents) must be responsible for spike repolarisation in honeybee projection neurons. Supporting evidence for different expressions of K^+ channels comes from immunohistochemical studies of the *Drosophila* brain showing that shaker channel proteins are highly expressed in the mushroom body neuropil, but not in the antennal lobes (Rogero et al., 1997). Furthermore, axons of motoneurons and mechanosensory neurons within the antennal nerve of the fly are shaker-immunoreactive, consistent with the presence of transient K^+ currents in antennal motoneurons in honeybees (Kloppenburg et al., 1999a).

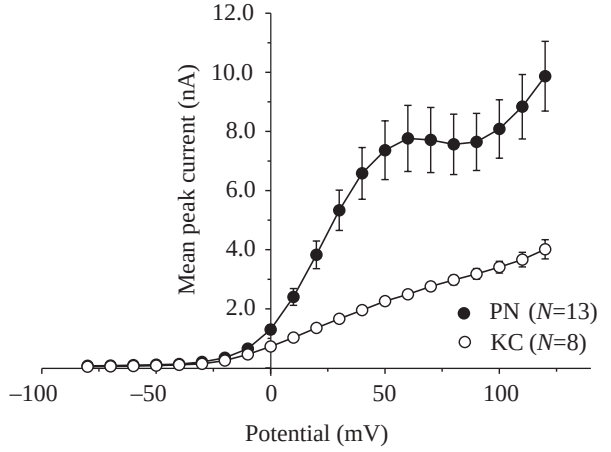

Fig. 6. Comparison of current–voltage relationships of K^+ currents of Kenyon cells (KC) and projection neurons (PN). Currents were recorded in external saline containing 100 nmol l^{-1} tetrodotoxin (TTX) and were elicited by command voltage pulses between –80 mV and +120 mV (increment 10 mV; preceded by a prepulse to –120 mV for 1 s; holding potential –80 mV; see pulse protocol in Fig. 5). Current amplitudes were measured at the peak of the transient current component (arrows in Fig. 5A) and averaged (values are means ± S.E.M.; the numbers of observations are indicated). Projection neurons express higher current amplitudes than Kenyon cells and show a pronounced N-shaped I-V curve at positive membrane potentials. The I-V curve of outward currents of Kenyon cells is rather linear between –20 and +120 mV.

Ca^{2+}-dependent K^+ currents have been described in a variety of insect neurons (e.g. Thomas, 1984; Nightingale and Pitman, 1989; David and Pitman, 1995; Grolleau and Lapied, 1995; Mills and Pitman, 1999; Hewes, 1999) (for reviews, see Saito and Wu, 1991; Wei et al., 1994; Grolleau and Lapied, 2000; Wicher et al., 2001). They may provide many functional roles within the nervous system, including spike repolarisation (e.g. Lapied et al., 1989) and afterhyper-polarisation (Saito and Wu, 1993; Hu et al., 2001). Ca^{2+}-dependent K^+ currents can be blocked by Ca^{2+} channel blockers (typically Cd^{2+} in insect neurons). This treatment reduced the amplitude of outward currents in projection neurons, but not in Kenyon cells. In addition projection neurons, which express voltage and Ca^{2+}-dependent K^+ currents, show a nonlinear I-V relationship at positive command potentials, because the K^+ current amplitude is influenced by the activation of voltage-sensitive Ca^{2+} channels. Assigning the honeybee Ca^{2+}-dependent K^+ current to any of the identified insect or vertebrate channels is currently not possible. It remains to be analysed whether the currents are both calcium- and voltage-dependent and whether honeybees express two separate Ca^{2+}-dependent K^+ channels as in DUM neurons of *Periplaneta* (Grolleau and Lapied, 1995) or *Drosophila* 'giant' neurons (Saito and Wu, 1991).

Probably all insect neurons express voltage-sensitive Ca^{2+} channels. These currents may contribute to action potential generation, synaptic transmission or neuromodulation (for reviews, see Jeziorski et al., 2000; Wicher et al., 2001). The voltage-sensitive Ca^{2+} currents of the honeybee projection neurons and Kenyon cells are similar (with respect to steady-state activation, Cd^{2+}-sensitivity and inactivation) to those described in other insect preparations, e.g. *Drosophila* (Byerly and Leung, 1988; Saito and Wu, 1993; Schmidt et al., 2000), *Periplaneta* (Grolleau and Lapied, 1996; Wicher and Penzlin, 1997; Mills and Pitman, 1997), *Manduca* (Hayashi and Levine, 1992), *Gryllus* (Kloppenburg and Hörner, 1998) and locusts (Laurent et al., 1993; Pearson et al., 1993). They activate rapidly and show a slow inactivation. The functional properties

of the Ca^{2+} currents of Kenyon cells and projection neurons presented here are thus consistent with earlier descriptions of Kenyon cells (Schäfer et al., 1994). The Ca^{2+} current densities of Kenyon cells and projection neurons are similar, which implies that the observed differences in Ca^{2+}-dependent K^+ currents are not due to differing densities of Ca^{2+} channels, but may indeed represent differential expression of Ca^{2+}-dependent K^+ channel proteins in Kenyon cells and projection neurons.

Although the present results are largely consistent with earlier investigations (Schäfer et al., 1994), there are differences as well. The finding that Kenyon cells did not show

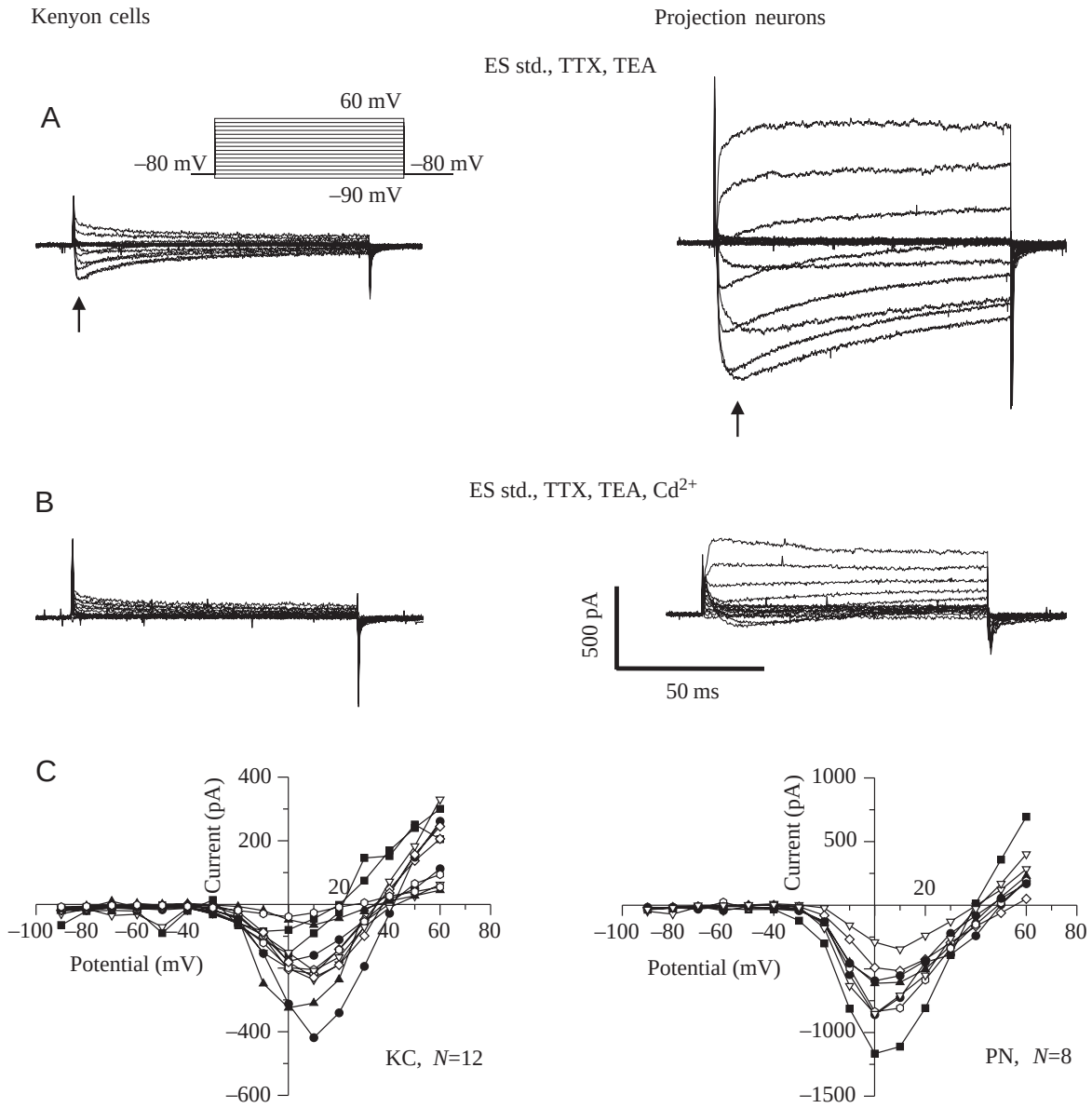

Fig. 7. Currents through voltage-sensitive Ca^{2+} channels. (A) Typical currents through Ca^{2+} channels of Kenyon cells (left) and projection neurons (right) show different amplitudes of inward currents. Currents were elicited by depolarizing voltage pulses (–90 to +60 mV, increment 10 mV; duration 100 ms; holding potential –80 mV); protocol (inset). Tetraethylammonium chloride (TEA, 10 mmol l^{-1}) and 100 nmol l^{-1} TTX were added to the external standard saline (ES std., see Materials and methods). To block K^+ outward currents further, the internal saline contained CsF (40 mmol l^{-1}), Cs-gluconate (83 mmol l^{-1}), Cs-EGTA (10 mmol l^{-1}) and TEA-Cl instead of the corresponding K^+ salts (cf. Materials and methods section). (B) Addition of 50 µmol l^{-1} $CdCl_2$ (Cd^{2+}) blocked the voltage-sensitive Ca^{2+} currents completely in Kenyon cells. A small residual Cd^{2+}-insensitive current remained unblocked in projection neurons. The Cd^{2+} block was irreversible even after excessive periods of wash (up to 30 min). (C) Current–voltage relationships of the currents through voltage-sensitive Ca^{2+} currents of all measured neurons show different amplitudes of peak inward currents (measured at the time point indicated by the arrow in A) and diversity of Ca^{2+} currents between neurons of a given type. The amplitudes of the peak currents are higher in projection neurons (PN, right) than in those of Kenyon cells (KC, left). However, the voltage-dependencies of the currents and the variability of the current amplitudes at the various potentials (–90 to +60 mV) appear to be similar.

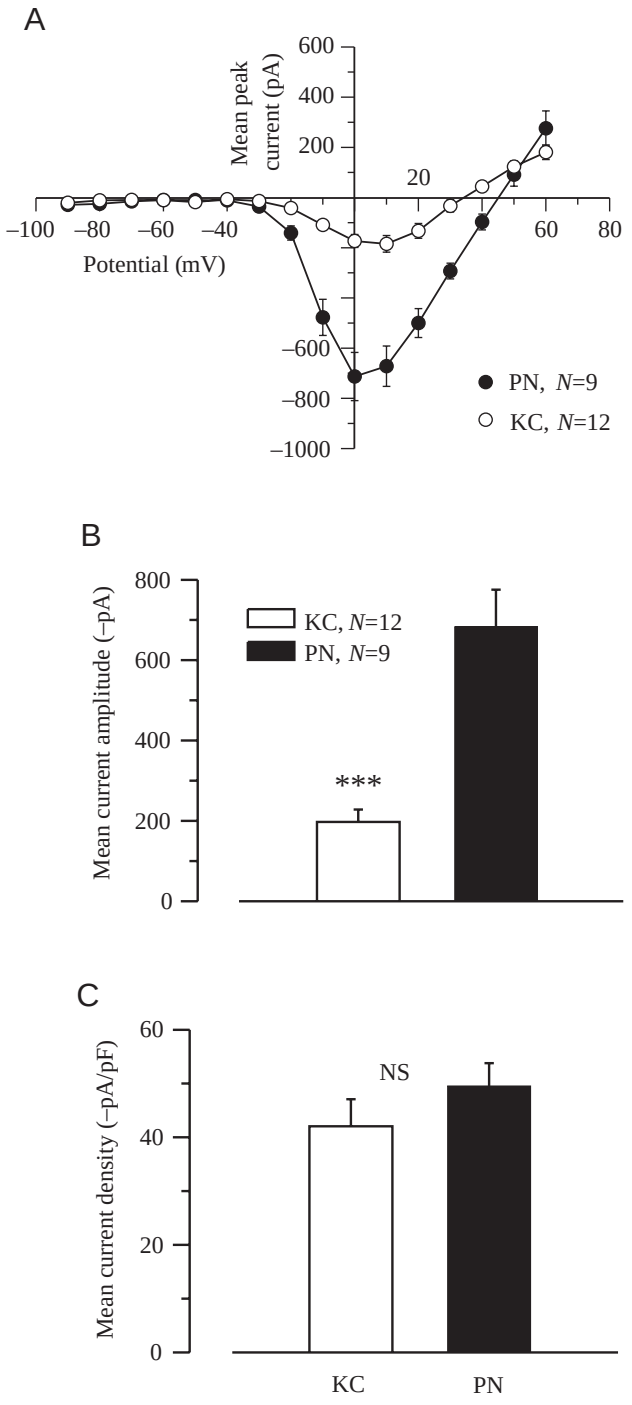

Fig. 8. Comparison of Ca^{2+} currents of Kenyon cells and projection neurons. (A) The voltage-dependencies of Ca^{2+} currents are similar, but projection neurons (PN) show higher current amplitudes than Kenyon cells (KC). Values are means ± S.E.M. of the peak Ca^{2+} current amplitudes measured at the time point indicated by the arrows in Fig. 7A (numbers of observations are indicated) at the respective pulse potential (pulse protocol is given in Fig. 7). (B) Mean peak current amplitudes are higher in projection neurons than in Kenyon cells (P<0.001). (C) Ca^{2+} current densities (–pA/pF) do not differ significantly (NS). The cell capacitances were measured for each cell using the capacitance compensation of the patch amplifier. All values are means ± S.E.M.

pronounced calcium-dependent K^+ currents, contradicts the report of these currents by Schäfer et al. (1994). What could be the reasons for this discrepancy? We exclude differences in Ca^{2+} channel expression between both studies, because the Ca^{2+} currents are very similar with respect to activation threshold (approximately –40 mV) and peak current amplitudes (means –160 pA and –197 pA). The culture conditions have been changed since the study by Schäfer et al. (1994), e.g. the components and pH of the medium. However, it is implausible that these changes abolish Ca^{2+}-dependent K^+ currents only in Kenyon cells and not in projection neurons, because both neuron types were cultured and measured in parallel under the same conditions. The recordings by Schäfer et al. (1994) were performed solely from the somata, because only cells without any processes were used, and the neurons were cultured for only 12–36 h. In the present study neurons were allowed to grow for 3–6 days and formed small neurites. Therefore, the whole cell currents may comprise somatic and neuritic currents. Accordingly, Kenyon cells may express somatic, but not neuritic Ca^{2+}-dependent K^+ currents. It is interesting to note here that Pelz et al. (1999) also observed differences in the pharmacology and kinetics of the A type K^+ current as compared to Schäfer et al. (1994), but the ultimate reasons for these differences remain unclear.

Functional roles of differential current expression

Differences in the ionic currents between Kenyon cells and projection neurons indicate that a specific expression pattern is maintained throughout the culturing procedure and for several days *in vitro*. Therefore, the observed differences may in fact represent physiological differences of these neuron types *in vivo*. In the living honeybee brain neither the function nor the dendritic or axonal localization of the various voltage-sensitive ionic currents has yet been satisfyingly unraveled. Both Kenyon cells and projection neurons generate action potentials (Homberg, 1984; Hammer and Menzel, 1995; Abel et al., 2001; Müller et al., 2002), but differ with respect to the outward currents, which probably mediate spike repolarisation. Thus, different ionic currents may interact during spike generation in the two neuron classes. Both the antennal lobe and the mushroom body are involved in olfactory learning and memory formation (Masuhr and Menzel, 1972; Hammer and Menzel, 1998; Menzel, 1999) and both are innervated by modulatory octopaminergic neurons (Hammer, 1993, 1997; Kreissl et al., 1994). Additional work is required to reveal the functional significance of the differential expression of K^+ currents of the different neuron types within the central olfactory pathway of the honeybee and whether these currents are differentially modulated during olfactory learning.

The author wishes to thank Holger Anlauf and Marion Ganz for skilful technical assistance with neuron staining protocols and cell culture techniques. I am grateful to Dr Einar Heidel for critically reading the manuscript, Mary Wurm for help with the English version, and Dr Randolf Menzel for continuous support and many valuable discussions

at all steps of this work. This work was supported by the Deutsche Forschungsgemeinschaft, SFB 515/C5.

References

Abel, R., Rybak, J. and Menzel, R. (2001). Structure and response patterns of olfactory interneurons in the honeybee, *Apis mellifera*. *J. Comp. Neurol.* **437**, 363-383.

Benkenstein, C., Schmidt, M. and Gewecke, M. (1999). Voltage-activated whole-cell K^+ currents in lamina cells of the desert locust *Schistocerca gregaria*. *J. Exp. Biol.* **202**, 1939-1951.

Bicker, G., Schäfer, S. and Kingan, T. G. (1985). Mushroom body feedback interneurons in the honeybee show GABA-like immunoreactivity. *Brain Res.* **360**, 394-397.

Byerly, L. and Leung, H.-T. (1988). Ionic currents of Drosophila neurons in embryonic cultures. *J. Neurosci.* **8**, 4379-4393.

David, J. A. and Pitman, R. M. (1995). Calcium and potassium currents in the fast coxal depressor motor neuron of the cockroach *Periplaneta americana*. *J. Neurophysiol.* **74**, 2043-2050.

Deglise, P., Grünewald, B. and Gauthier, M. (2002). The insecticide imidacloprid is a partial agonist of the nicotinic receptor of honeybee Kenyon cells. *Neurosci. Lett.* **321**, 13-16.

Delgado, R., Davis, R. L., Bono, M. R., Latorre, R. and Labarca, P. (1998). Outward currents in Drosophila larval neurons: dunce lacks a maintained outward current component downregulated by cAMP. *J. Neurosci.* **18**, 1399-1407.

Devaud, J. M., Quenet, B., Gascuel, J. and Masson, C. (1994). A morphometric classification of pupal honeybee antennal lobe neurones in culture. *NeuroRep.* **6**, 214-218.

Dugladze, T., Heinemann, U. and Gloveli, T. (2001). Entorhinal cortex projection cells to the hippocampal formation in vitro. *Brain Res.* **905**, 224-231.

Erber, J., Homberg, U. and Gronenberg, W. (1987). Functional roles of the mushroom bodies in insects. In *Arthropod brain: Its Evolution, Development, Structure and Functions* (ed. A. P. Gupta), pp. 485-511. New York: John Wiley and Sons.

Erber, J., Masuhr, T. and Menzel, R. (1980). Localization of short-term memory in the brain of the bee, *Apis mellifera*. *Physiol. Entomol.* **5**, 343-358.

Fiala, A., Müller, U. and Menzel, R. (1999). Reversible downregulation of protein kinase A during olfactory learning using antisense technique impairs long-term memory formation in the honeybee, *Apis mellifera*. *J. Neurosci.* **19**, 10125-10134.

Fonta, C., Sun, X.-J. and Masson, C. (1993). Morphology and spatial distribution of bee antennal lobe interneurones responsive to odours. *Chem. Senses* **18**, 101-119.

Gascuel, J. and Masson, C. (1991a). A quantitative ultrastructural study of the honeybee antennal lobe. *Tissue Cell* **23**, 341-355.

Gascuel, J. and Masson, C. (1991b). Developmental study of afferented and deafferented bee antennal lobes. *J. Neurobiol.* **22**, 795-810.

Goldberg, F., Grünewald, B., Rosenboom, H. and Menzel, R. (1999). Nicotinic acetylcholine currents of cultured Kenyon cells from the mushroom bodies of the honey bee *Apis mellifera*. *J. Physiol.* **514**, 759-768.

Grolleau, F. and Lapied, B. (1995). Separation and identification of multiple potassium currents regulating the pacemaker activity of insect neurosecretory cells (DUM neurons). *J. Neurophysiol.* **73**, 160-171.

Grolleau, F. and Lapied, B. (1996). Two distinct low-voltage-activated Ca^{2+} currents contribute to the pacemaker mechanism in cockroach dorsal unpaired median neurons. *J. Neurophysiol.* **76**, 963-976.

Grolleau, F. and Lapied, B. (2000). Dorsal unpaired median neurones in the insect central nervous system: towards a better understanding of the ionic mechanisms underlying spontaneous electrical activity. *J. Exp. Biol.* **203**, 1633-1648.

Grünbaum, L. and Müller, U. (1998). Induction of a specific olfactory memory leads to a long-lasting activation of protein kinase C in the antennal lobe of the honeybee. *J. Neurosci.* **18**, 4384-4392.

Grünewald, B. (1999a). Morphology of feedback neurons in the mushroom body of the honeybee, *Apis mellifera*. *J. Comp. Neurol.* **404**, 114-126.

Grünewald, B. (1999b). Physiological properties and response modulations of mushroom body feedback neurons during olfactory learning in the honeybee, *Apis mellifera*. *J. Comp. Physiol. A* **185**, 565-576.

Hamill, O. P., Neher, E., Marty, A., Sakman, B. and Sigworth, F. J. (1981). Improved patch-clamp techniques for high-resolution current recording from cells and cell-free membrane patches. *Pflügers Arch. Eur. J. Physiol.* **391**, 85-100.

Hammer, M. (1993). An identified neuron mediates the unconditioned stimulus in associative olfactory learning in honeybees. *Nature* **366**, 59-63.

Hammer, M. (1997). The neural basis of associative reward learning in honeybees. *Trends Neurosci.* **20**, 245-252.

Hammer, M. and Menzel, R. (1995). Learning and memory in the honeybee. *J. Neurosci.* **15**, 1617-1630.

Hammer, M. and Menzel, R. (1998). Multiple sites of associative odor learning as revealed by local brain microinjections of octopamine in honeybees. *Learn. Mem.* **5**, 146-156.

Hayashi, J. H. and Hildebrand, J. G. (1990). Insect olfactory neurons in vitro: morphological and physiological characterization of cells from the developing antennal lobes of *Manduca sexta*. *J. Neurosci.* **10**, 848-859.

Hayashi, J. H. and Levine, R. B. (1992). Calcium and potassium currents in leg motoneurons during postembryonic development in the hawkmoth *Manduca sexta*. *J. Exp. Biol.* **171**, 15-42.

Hewes, R. S. (1999). Voltage-dependent ionic currents in the ventromedial eclosion hormone neurons of *Manduca sexta*. *J. Exp. Biol.* **202**, 2371-2383.

Hildebrandt, H. and Müller, U. (1995). Octopamine mediates rapid stimulation of protein kinase A in the antennal lobe of honeybees. *J. Neurobiol.* **27**, 44-50.

Homberg, U. (1984). Processing of antennal information in extrinsic mushroom body neurons of the bee brain. *J. Comp. Physiol. A* **154**, 825-836.

Hu, H., Shao, L.-R., Chavoshy, S., Gu, N., Trieb, M., Behrens, R., Laaske, P., Pongs, O., Knaus, H. G., Ottersen, O. P. and Storm, J. F. (2001). Presynaptic Ca^{2+}-activated K^+ channels in glutamatergic hippocampal terminals and their role in spike repolarization and regulation of transmitter release. *J. Neurosci. Meth.* **21**, 9585-9597.

Ikeno, H. and Usui, S. (1999). Mathematical description of ionic currents of the Kenyon cell in the mushroom body of honeybee. *Neurocomputing* **26-27**, 177-184.

Jeziorski, M. C., Greenberg, R. M. and Anderson, P. A. (2000). The molecular biology of invertebrate voltage-gated Ca^{2+} channels. *J. Exp. Biol.* **203**, 841-856.

Joerges, J., Küttner, A., Galizia, C. G. and Menzel, R. (1997). Representations of odours and odour mixtures visualized in the honeybee brain. *Nature* **387**, 285-288.

Kenyon, C. F. (1896). The brain of the bee. A preliminary contribution to the morphology of the nervous system of the arthropoda. *J. Comp. Neurol.* **6**, 133-210.

Kirchhof, B. S. and Mercer, A. R. (1997). Antennal lobe neurons of the honey bee, *Apis mellifera*, express a D2-like dopamine receptor in vitro. *J. Comp. Neurol.* **383**, 189-198.

Kloppenburg, P. and Hörner, M. (1998). Voltage-activated currents in identified giant interneurons isolated from adult crickets *Gryllus bimaculatus*. *J. Exp. Biol.* **201**, 2529-2541.

Kloppenburg, P., Kirchhof, B. S. and Mercer, A. R. (1999a). Voltage-activated currents from adult honeybee (*Apis mellifera*) antennal motor neurons recorded in vitro and in situ. *J. Neurophysiol.* **81**, 39-48.

Kloppenburg, P., Levini, R. M. and Harris-Warrick, R. M. (1999b). Dopamine modulates two potassium currents and inhibits the intrinsic firing properties of an identified motor neuron in a central pattern generator network. *J. Neurophysiol.* **81**, 29-38.

Kreissl, S. and Bicker, G. (1992). Dissociated neurons of the pupal honeybee brain in cell culture. *J. Neurocytol.* **21**, 545-556.

Kreissl, S., Eichmüller, S., Bicker, G., Rapus, J. and Eckert, M. (1994). Octopamine-like immunoreactivity in the brain and subesophageal ganglion of the honeybee. *J. Comp. Neurol.* **348**, 583-595.

Lapied, B., Pelhate, M. and Pelhate, M. (1989). Ionic species involved in the electrical activity of single adult aminergic neurones isolated from the sixth abdominal ganglion of the cockroach *Periplaneta americana*. *J. Exp. Biol.* **144**, 535-549.

Laurent, G., Seymour-Laurent, K. J. and Johnson, K. (1993). Dendritic excitability and a voltage-gated calcium current in locust nonspiking local interneurons. *J. Neurophysiol.* **69**, 1484-1498.

Masuhr, T. and Menzel, R. (1972). Learning experiments on the use of sidespecific information in the olfactory and visual system in the honeybee (*Apis mellifica*). In *Information Processing in the Visual Systems of Arthropods* (ed. R. Wehner), pp. 315-322. Berlin-Heidelberg-New York: Springer.

Mauelshagen, J. (1993). Neural correlates of olfactory learning paradigms in an identified neuron in the honeybee brain. *J. Neurophysiol.* **69**, 609-625.

Menzel, R. (1999). Memory dynamics in the honeybee. *J. Comp. Physiol. A* **185**, 323-340.

Menzel, R. (2001). Searching for the memory trace in a mini-brain, the honeybee. *Learn. Mem.* **8**, 53-62.

Menzel, R. and Müller, U. (1996). Learning and memory in honeybees: from behaviour to neural substrates. *Ann. Rev. Neurosci.* **19**, 379-404.

Mercer, A. R. and Hildebrand, J. G. (2002a). Developmental changes in the density of ionic currents in antennal-lobe neurons of the sphinx moth, *Manduca sexta*. *J. Neurophysiol.* **87**, 2664-2675.

Mercer, A. R. and Hildebrand, J. G. (2002b). Developmental changes in the electrophysiological properties and response characteristics of *Manduca sexta* antennal-lobe neurons. *J. Neurophysiol.* **87**, 2650-2663.

Mills, A. and Pitman, R. M. (1997). Electrical properties of a cockroach motor neuron soma depend on different characteristics of individual Ca components. *J. Physiol.* **78**, 2455-2466.

Mills, J. D. and Pitman, R. M. (1999). Contribution of potassium conductances to a time-dependent transition in electrical properties of a cockroach motoneuron soma. *J. Neurophysiol.* **81**, 2253-2266.

Mobbs, P. G. (1982). The brain of the honeybee *Apis mellifera*. I. The connections and spatial organization of the mushroom bodies. *Phil. Trans. R. Soc. Lond. B.* **298**, 309-354.

Mobbs, P. G. (1985). Brain structure. In *Comprehensive Insect Physiology, Biochemistry, and Pharmacology*, vol. 5 (ed. G. A. Kerkut and L. I. Gilbert), pp. 299-370. Oxford: Pergamon Press.

Müller, D., Abel, R., Brandt, R., and Zöckler, M. (2002). Differential parallel processing of olfactory information in the honeybee, *Apis mellifera* L. *J. Comp. Physiol. A* **188**, 359-370.

Müller, U. (1996). Inhibition of nitric oxide synthase impairs a distinct form of long-term memory in the honeybee *Apis mellifera*. *Neuron* **16**, 541-549.

Müller, U. (2000). Prolonged activation of cAMP-dependent protein kinase during conditioning induces long-term memory in honeybees. *Neuron* **27**, 159-168.

Nightingale, W. D. and Pitman, R. M. (1989). Ionic currents in the soma of an identified cockroach motoneurone recorded under voltage-clamp. *Comp. Biochem. Physiol.* **93A**, 85-93.

Oland, L. A. and Hayashi, J. H. (1993). Effects of the steroid hormone 20-hydroxyectysone and prior sensory input on the survival and growth of Moth central olfactory neurons in vitro. *J. Neurobiol.* **24**, 1170-1186.

Oland, L. A., Müller, T., Kettenmann, H. and Hayashi, J. (1996). Preparation of primary cultures and acute slices of the nervous system of the moth *Manduca sexta*. *J. Neurosci. Methods* **69**, 103-112.

Pearson, H. A., Lees, G. and Wray, D. (1993). Calcium channel currents in neurones from locust (*Schistocerca gregaria*) thoracalic ganglia. *J. Exp. Biol.* **177**, 201-221.

Pelz, C., Jander, J., Rosenboom, H., Hammer, M. and Menzel, R. (1999). I_A in Kenyon cells of the mushroom body of honeybees resembles shaker currents: kinetics, modulation by K^+, and simulation. *J. Neurophysiol.* **81**, 1749-1759.

Rogero, O., Hämmerle, B. and Tejedor, F. J. (1997). Diverse expression and distribution of Shaker potassium channels during the development of the Drosophila nervous system. *J. Neurosci.* **17**, 5108-5118.

Rybak, J. and Menzel, R. (1993). Anatomy of the mushroom bodies in the honey bee brain: the neuronal connections of the alpha-lobe. *J. Comp. Neurol.* **334**, 444-465.

Sachse, S., Rappert, A. and Galizia, C. G. (1999). The spatial representation of chemical structures in the antennal lobe of honeybees: steps towards the olfactory code. *Eur. J. Neurosci.* **11**, 3970-3982.

Saito, M. and Wu, C.-F. (1991). Expression of ion channels and mutational effects in giant Drosophila neurons differentiated from cell division-arrested embryonic neuroblasts. *J. Neurosci.* **11**, 2135-2150.

Saito, M. and Wu, C.-F. (1993). Ionic channels in cultured Drosophila neurons. *EXS* **63**, 366-389.

Schäfer, S., Rosenboom, H. and Menzel, R. (1994). Ionic currents of Kenyon cells from the mushroom body of the honeybee. *J. Neurosci.* **14**, 4600-4612.

Schmidt, H., Lüer, K., Hevers, W. and Technau, G. M. (2000). Ionic currents of Drosophila embryonic neurons derived from selectively cultured CNS midline precursors. *J. Neurobiol.* **44**, 392-413.

Schröter, U. and Malun, D. (2000). Formation of antennal lobe and mushroom body neuropils during metamorphosis in the honeybee, Apis mellifera. *J. Comp. Neurol.* **422**, 229-245.

Stopfer, M., Bhagavan, S., Smith, B. H., and Laurent, G. (1997). Impaired odour discrimination on desynchronization of odour-encoding neural assemblies. *Nature* **390**, 70-74.

Tanouye, M. A. and Ferrus, A. (1985). Action potentials in normal and shaker mutant Drosophila. *J. Neurogenet.* **2**, 253-271.

Thomas, M. V. (1984). Voltage-clamp analysis of a calcium-mediated potassium conductance in cockroach (*Periplaneta americana*) central neurones. *J. Physiol.* **350**, 159-178.

Wei, A., Solaro, C., Lingle, C. and Salkoff, L. (1994). Calcium sensitivity of BK-type KCa channels determined by a separable domain. *Neuron* **13**, 671-681.

Wicher, D. and Penzlin, H. (1997). Ca^{2+} currents in central insect neurons: electrophysiological and pharmacological properties. *J. Neurophysiol.* **77**, 186-199.

Wicher, D., Walther, C. and Wicher, C. (2001). Non-synaptic ion channels in insects – basic properties of currents and their modulation in neurons and skeletal muscles. *Prog. Neurobiol.* **64**, 431-525.